



Minerva Access is the Institutional Repository of The University of Melbourne

Author/s:

Zhang, Y;Skinner, JP;Chong, MMW

Title:

Expression of the miR-17~92a cluster of microRNAs by regulatory T cells controls blood glucose homeostasis

Date:

2022-02-01

Citation:

Zhang, Y., Skinner, J. P. & Chong, M. M. W. (2022). Expression of the miR-17~92a cluster of microRNAs by regulatory T cells controls blood glucose homeostasis. *Immunology and Cell Biology*, 100 (2), pp.101-111. <https://doi.org/10.1111/imcb.12513>.

Persistent Link:

<https://hdl.handle.net/11343/311211>

1

2 ASSOCIATE PROFESSOR MARK CHONG (Orcid ID : 0000-0002-3701-7397)

3

4

5 Article type : Original Article

6

7

8 **Expression of the miR-17~92a cluster of microRNAs by regulatory T cells controls blood**
9 **glucose homeostasis**

10

11 Yangnan Zhang^{1,2}, Jarrod P Skinner¹ & Mark MW Chong^{1,2,*}

12

13 ¹ St Vincent's Institute of Medical Research, Fitzroy, VIC, Australia

14 ² Department of Medicine (St Vincent's), University of Melbourne, Fitzroy, VIC, Australia

15

16 * Corresponding author

17 Email: mchong@svi.edu.au

18 Postal address: 9 Princes Street, Fitzroy, VIC 3065, Australia

19

20 Running title: Treg microRNAs regulate blood glucose

This is the author manuscript accepted for publication and has undergone full peer review but has not been through the copyediting, typesetting, pagination and proofreading process, which may lead to differences between this version and the [Version of Record](#). Please cite this article as [doi: 10.1111/IMCB.12513](https://doi.org/10.1111/IMCB.12513)

This article is protected by copyright. All rights reserved

21 **ABSTRACT**

22 Regulatory T cells (Tregs) are a specialised immune cell type that plays important roles in
23 regulating immune responses. However, those found in adipose tissue, particularly visceral adipose
24 tissue (VAT), have also been shown to exert metabolic regulatory functions. In this study, we
25 investigate the requirement of the miR-17~92a cluster of microRNAs in VAT Tregs and the impact
26 on blood glucose. This cluster of microRNAs is one that we previously showed to be important for
27 the fitness of Tregs found in secondary lymphoid organs. We found that male mice with Treg-
28 specific miR-17~92a deficiency are resistant to impaired glucose tolerance induced by a high-fat
29 diet. However, high-fat feeding still impaired glucose tolerance in female mice with Treg-specific
30 miR-17~92a deficiency. There was an increase in KLRG1⁻ naïve Tregs and a loss of KLRG1⁺
31 terminally differentiated Tregs in the VAT of Treg-specific miR-17~92a deficient male mice but
32 not female mice. The protection of male mice from high-fat feeding was also associated with
33 increased IL-10 and reduced IFN γ expression by conventional CD4⁺ T cells and reduced IL-2
34 expression by both CD4⁺ and CD8⁺ T cells in the VAT. Together this suggests that expression of
35 miR-17~92a by VAT Tregs regulates the effector phenotype of conventional T cells and in turn the
36 metabolic function of adipose tissue and blood glucose homeostasis.

37

38 **KEYWORDS**

39 MicroRNA, regulatory T cells, adipose tissue, blood glucose

41 **INTRODUCTION**

42 Adipose tissue is the main energy store of the body and is important for the regulation of metabolic
43 homeostasis. It consists of adipocytes, which stores fat, surrounded by a matrix of dispersed
44 immature adipocytes, immune cells and other cell types ¹. The immune compartment is particularly
45 diverse, which includes macrophages, dendritic cells and T cells, and under normal conditions have
46 roles in the elimination of apoptotic cell debris and the regulation of adipose tissue function ².

47

48 Regulatory T cells (Tregs) are a specialised lineage of T cells that is critical for immune
49 homeostasis by regulating the activation and function of other immune cells. They are characterised
50 by the expression of the lineage-defining transcription factor FOXP3 ³. Mutations in the *Foxp3* gene
51 are associated with Treg deficiency and severe systemic autoimmune disorders ⁴. There are two
52 sources of Tregs in the body. Those that develop within the thymus from CD4⁺CD8⁺ double
53 positive thymocytes are known as thymic or natural Tregs ⁵. In addition, Tregs can differentiate
54 from naïve conventional CD4⁺ T cells in peripheral tissues following appropriate antigenic
55 stimulation and these are known as induced Tregs ⁵.

56

57 The Tregs found in adipose tissue and particularly visceral adipose tissue (VAT), have critical roles
58 in regulating metabolic homeostasis ³. Specific depletion of these cells in mice induces local
59 inflammation, insulin resistance and impaired glucose tolerance ⁶. Gain-of-function experiments in
60 which mice are treated with the cytokine IL-10, which is normally secreted by adipose Tregs, or
61 with IL-2 plus anti-IL-2 antibody to expand Treg numbers, both lead to improved insulin sensitivity
62 and glucose tolerance following a high-fat diet (HFD) ^{6,7}.

63

64 The frequency and function of adipose-resident Tregs appear to be influenced by a range of factors.
65 Metabolic status is one. The number of Tregs found in the VAT of male mice is reduced the ob/ob
66 and Ay/a mouse models of obesity ^{6,8}. VAT Tregs are also lost in wildtype male mice fed a HFD.
67 These findings point to another factor, sexual dimorphism. VAT Tregs from male and female mice
68 display distinct transcriptional profiles and these are influenced by sex hormones, which ultimately
69 translates to different responses to high caloric intake and adipose inflammation ^{9,10}. Age is another
70 factor. The number of Tregs found in adipose tissue increases with age but, counterintuitively, this
71 increase appears to contribute to the development of age-associated insulin resistance ¹¹. Selective
72 depletion of adipose-resident Tregs attenuates many of the hallmarks of age-associated metabolic
73 dysregulation, such as insulin resistance and impaired glucose tolerance ¹¹.

74

75 Adipose-resident Tregs display a transcriptional profile that distinguishes them those found in
76 lymphoid organs ¹². Moreover, they are also distinguishable from Tregs found in other non-
77 lymphoid tissues. The resident Tregs found in different tissues have been shown to express unique
78 cell surface markers, transcription factors, effector molecules and distinct repertoires of T cell
79 receptors ¹². VAT Tregs distinctly express the transcription factor PPAR- γ and a unique pattern of
80 chemokine receptors⁶. PPAR- γ is required for the localization and function of adipose-resident
81 Tregs ¹³. PPAR- γ is also essential for the differentiation and function of adipocytes ¹⁴. This suggest
82 that the identity of VAT Tregs may be determined by the local environment in which they are
83 found. It has been shown that this is at least partly dependent on the adipose-resident macrophages
84 ¹⁵. Id2, IRF4 and BATF are other transcription factors that are highly expressed in adipose-resident
85 Tregs and have been shown to be important for their accumulation and function within adipose
86 tissue ¹⁶⁻¹⁸. These appear to regulate the expression of the IL-33R, and IL-33 is a cytokine that is
87 important for differentiation and maintenance of adipose Tregs ¹⁸.

88
89 While recent studies have revealed much about the transcriptional networks in adipose-resident
90 Tregs, there is still much that we do not understand about the molecular pathways that govern
91 the identity and function of these cells. MicroRNAs (miRNAs) may have a role, which are short
92 ~22 nucleotide non-coding RNAs that inhibit the translation and stability of protein-coding
93 messenger (m)RNAs ¹⁹. The miRNA pathway is critical for the development and function of Tregs,
94 at least those found in lymphoid organs. Treg-specific deletion of the genes encoding DROSHA or
95 DICER, the two RNase III enzymes that are essential for the biogenesis of microRNAs, results in
96 uncontrolled lethal inflammation in mice ²⁰⁻²², a phenotype that is identical to mice with FOXP3
97 deficiency. Moreover, FOXP3 drives the transcription of specific miRNA genes in Tregs,
98 suggesting that FOXP3 exerts at least some of its functions via miRNAs ²³. Tregs highly express a
99 number of miRNA species. These include those from the well-characterized miR-17~92a miRNA
100 gene cluster ²⁴. We and others previously showed that this cluster of miRNAs is critical for the
101 homeostasis of lymphoid Tregs by regulating the proliferation, apoptosis and effector function of
102 these cells ²⁵⁻²⁷.

103
104 While it is clear that the miRNA pathway is critical for the development and function of lymphoid
105 Tregs, it remains unknown whether this pathway is also important in the adipose-resident or other
106 tissue-resident Tregs. In this study, we investigate the requirement of the miR-17~92a cluster in
107 adipose-resident Tregs and the influence on blood glucose homeostasis.

108 **RESULTS**

109 **Treg-specific miR-17~92a deficiency protects male mice from impaired glucose tolerance**
110 **induced by high-fat feeding**

111 To investigate whether miR-17~92a is required for the function of adipose-resident Tregs, we
112 analysed conditional *Mir17hg^{lox}* mice harbouring a *Foxp3^{IRE5-Cre}* knockin (hereinafter referred to as
113 *Mir17hg Foxp3-cre* mice), which results in deletion of the *Mir17hg* gene only in FOXP3-expressing
114 cells. This deletion occurs in all Tregs, including those found in adipose tissue and secondary
115 lymphoid organs²⁶. The *Foxp3* gene is located on the X-chromosome. To account for random X-
116 chromosome inactivation, female mice were maintained as *Mir17hg^{lox/lox} Foxp3^{IRE5-Cre/IRE5-Cre}*
117 (homozygous for both alleles), while male mice were maintained as *Mir17hg^{lox/lox} Foxp3^{IRE5-Cre/Y}*
118 (hemizygous for the Cre knockin). *Mir17hg^{lox/lox} Foxp3^{IRE5-Cre/Y}* male mice were mated with
119 wildtype female mice to produce control *Mir17hg^{lox/+} Foxp3^{+/Y}* male and *Mir17hg^{lox/+} Foxp3^{IRE5-}*
120 *Cre/+* female mice. We previously showed that while miR-17~92a is important for the homeostasis
121 of lymphoid Tregs, the lymphoid organs of *Mir17hg Foxp3-cre* mice only display minor
122 perturbations. Importantly they do not display any obvious signs of autoimmunity²⁶ and thus, the
123 metabolic status of young animals can be assessed.

124
125 *Mir17hg Foxp3-cre* and control mice were fed on normal chow or HFD for eight weeks from
126 weaning then subjected to glucose tolerance testing. On a normal chow diet, *Mir17hg Foxp3-cre*
127 male and female mice were indistinguishable from control mice (Figure 1a–c). Chow-fed *Mir17hg*
128 *Foxp3-cre* mice cleared glucose at the same rate as control mice. However, while high-fat feeding
129 impaired the response of control male mice, this impairment was not observed in *Mir17hg Foxp3-*
130 *cre* male mice (Figure 1a–c). HFD-fed *Mir17hg Foxp3-cre* male mice reached a lower maximal
131 blood glucose than HFD-fed control male mice and cleared the glucose over the 2 h challenge. In
132 fact, HFD-fed *Mir17hg Foxp3-cre* male mice cleared glucose with the same efficiency as chow-fed
133 mice. HFD-fed control male mice did not return to baseline blood glucose levels within the course
134 of the challenge.

135
136 Interestingly, this protection from high-fat feeding was not observed in *Mir17hg Foxp3-cre* female
137 mice (Figure 1a, c). Their response was equally impaired as control female mice. Thus, expression
138 of the miR-17~92a cluster of miRNAs plays an important modulatory function in Tregs and the
139 regulation of blood glucose homeostasis but only in males.

140
141 *Mir17hg Foxp3-cre* male mice fed on a HFD were found to weigh the same as those fed on normal
142 chow diet, whereas control male and female mice fed a HFD were statistically heavier than those

143 fed on a normal chow diet (Supplementary figure 1). There was also a trend for HFD-fed Mir17hg
144 Foxp3-cre female mice to be heavier than those fed a normal chow diet.

145

146 **Treg-specific miR-17~92a deficiency results in a loss of peripheral-induced Tregs but not**
147 **thymic-derived Tregs in the VAT of male mice**

148 It is the Tregs found in VAT that play a critical role in metabolic homeostasis and increasing their
149 numbers or function improves glucose tolerance following HFD-feeding^{6,7}. We thus analysed the
150 VAT of Mir17hg Foxp3-cre mice (on a normal chow diet) for FOXP3⁺ Tregs (Supplementary
151 figure 2). As previously reported¹⁰, Tregs are more frequent in the VAT male mice than female
152 mice. However, there was no difference in either the frequency (Figure 2a) or absolute numbers
153 (Supplementary figure 3a) of VAT Tregs between Mir17hg Foxp3-cre and control mice of both
154 sexes.

155

156 Thymic-derived Tregs are distinguishable from peripheral induced Tregs by their expression of
157 neuropilin-1, also known as CD304²⁸. No difference in the frequency of CD304⁺FOXP3⁺ thymic
158 Tregs was observed between Mir17hg Foxp3-cre and control mice of both sexes, which accounted
159 for approximately two-thirds of the Tregs found in VAT (Figure 2b). However, there was a
160 significant reduction in the frequency of CD304⁺FOXP3⁺ peripheral induced Tregs in Mir17hg
161 Foxp3-cre male mice compared to controls (Figure 2c), while no difference was observed in female
162 mice.

163

164 **Treg-specific miR-17~92a deficiency alters the balance between naïve and terminally**
165 **differentiated Tregs in the VAT of male mice**

166 We next analysed the maturation status of the VAT Tregs. Expression of KLRG1 marks terminally
167 differentiated Tregs, while naïve Tregs lack expression of this marker²⁹. There was a reduction in
168 the frequency of KLRG1⁺ cells in both the thymic-derived (Figure 2d) and peripheral-induced
169 (Figure 2e) Treg compartments in Mir17hg Foxp3-cre male mice compared to control male mice,
170 and thus an increase in KLRG1⁻ naïve cells. This was somewhat unexpected because an increase in
171 terminally differentiated Tregs might have been predicted to correlate with the resistance to
172 impaired glucose homeostasis. The reduction in KLRG1⁺ cells in both thymic-derived and
173 peripheral-induced compartments means that miR-17~92a deficiency must be acting on at least two
174 distinct levels of VAT Treg maturation, the differentiation of induced Tregs and the terminal
175 differentiation of all Tregs, whether induced or thymic-derived. No difference in either Tregs
176 subpopulation were observed between Mir17hg Foxp3-cre and control female mice.

177

178 **Perturbations in Treg subpopulations in Treg-specific miR-17~92a deficient male mice are**
179 **maintained with HFD feeding**

180 We next analysed the impact of a HFD on VAT Treg populations in these mice. As expected ³⁰,
181 HFD-feeding resulted in a reduction in the total frequency of Tregs in the VAT mice, regardless of
182 miR-17~92a genotype (Figure 3a & Supplementary figure 3a). The altered proportions of Treg
183 subpopulations previously observed in chow-fed mice were maintained in these HFD-fed mice,
184 with Mir17hg Foxp3-cre male mice exhibiting a reduction in CD304-FOXP3⁺ peripheral induced
185 Tregs but not CD304⁺FOXP3⁺ thymic Tregs, as well as a reduction in KLRG1⁺ terminally cells in
186 both the thymic-derived and induced Treg compartments compared to control male mice (Figure
187 3b–e). Again, there was no statistical differences in Treg subpopulations between Mir17hg Foxp3-
188 cre and control female mice (Figure 3b–e).

189

190 **Conventional CD8⁺ T cells are increased in the VAT of Treg-specific miR-17~92a deficient**
191 **male mice**

192 The interplay between Tregs and other immune cells, particularly conventional CD4⁺ and CD8⁺ T
193 cells, within VAT is thought to be important for the regulation of adipose tissue function. Depletion
194 of Tregs results in an increase in CD4⁺ and CD8⁺ T cells numbers within VAT, while IFN γ from
195 Th1 CD4⁺ T cells inhibits Treg differentiation ³¹. We therefore investigated whether conventional T
196 cell populations in the VAT are affected by Treg-specific miR-17~92a deficiency in these mice.
197 The frequency (Figure 4a) or number (Supplementary figure 3b) of conventional (FOXP3⁻TCR β ⁺)
198 CD4⁺ T cells in the VAT of Mir17hg Foxp3-cre mice was no different to control mice in both males
199 and females, and whether fed on normal chow or HFD. However, there was an increase in
200 conventional CD8⁺ T cells in Mir17hg Foxp3-cre male mice whether fed on normal chow or HFD
201 (Figure 4b & Supplementary figure 3c). There was also a trend for an increase in CD8⁺ T cells in
202 Mir17hg Foxp3-cre female mice (Figure 4b & Supplementary figure 3c). Because miR-17~92a
203 deficiency is restricted only to Tregs, this increase in CD8⁺ T cells must be a downstream
204 consequent of altered Treg function.

205

206 **Increased IL-10 expression and decreased IFN γ expression by conventional CD4⁺ T cells in**
207 **the VAT of Treg-specific miR-17~92a deficient male mice**

208 We next investigated the phenotype of the conventional T cells in these mice. The VAT CD4⁺ T
209 cells of Mir17hg Foxp3-cre male mice were found to express higher levels of IL-10 and lower
210 levels of IFN γ than those of control mice, following high-fat feeding (Figure 5a, c). These cells also
211 expressed lower levels of IL-2. Interestingly, the VAT CD8⁺ T cells of Mir17hg Foxp3-cre male
212 mice expressed similar levels of IFN γ compared to control mice but lower levels of IL-2. In fact,

213 there was a substantial increase in the frequency of IFN γ ⁺IL-2⁻ CD8⁺ T cells in Mir17hg Foxp3-cre
214 male mice.

215

216 The VAT CD4⁺ T cells of Mir17hg Foxp3-cre female mice displayed similar expression of IL-10,
217 IL-2 and IFN γ compared to control mice (Figure 5b, c). However, like in their male counterparts,
218 there was a reduction in IL-2 expressing CD8⁺ T cells in Mir17hg Foxp3-cre female mice. There
219 was similarly a substantial increase in the frequency of IFN γ ⁺IL-2⁻ CD8⁺ T cells.

220

221 Finally, we found an increase in the frequency of KLRG1⁺ effector CD8⁺ T cells in the VAT of
222 both male and female Mir17hg Foxp3-cre mice compared to control mice (Figure 5d).

223

224 Together, these data suggest that a shift in the conventional CD4⁺ T cell compartment towards an
225 anti-inflammatory IL-10-expressing phenotype may potentially underlie the protection of Mir17hg
226 Foxp3-cre male mice from high-fat feeding. However, the phenotypic changes in conventional
227 CD8⁺ T cells are less likely to explain the resistance because the same changes were evident in
228 Mir17hg Foxp3-cre female mice.

229

230 **Ablation of the microRNA pathway in all T cells does not affect glucose tolerance**

231 Given that miR-17~92a deficiency in Tregs protected male mice from high-fat feeding, we
232 wondered if deficiency of the entire miRNA pathway might result in an even greater tolerance to
233 high fat. To investigate this, we analysed conditional *Drosha*^{lox} knockout mice harbouring a *CD4-*
234 *cre* transgene (hereinafter referred to as *Drosha* CD4-cre mice), which deletes the *Drosha* gene at
235 the CD4⁺CD8⁺ stage in T cell development. This results in DROSHA deficiency in all $\alpha\beta$ T cells,
236 include FOXP3⁺ Tregs²⁰. These mice also harbour a *FOXP3*^{IRES-GFP} knockin³² that allows the
237 identification of Tregs by GFP expression. Unlike *Drosha*^{lox/lox} *FOXP3*^{IRES-Cre/IRES-Cre} mice, in which
238 deletion is restricted only to Tregs, these mice with DROSHA deficiency in all T cells survive to
239 adulthood and do not develop obvious disease until much later in life, typically 6 to 9 months of age
240²⁰. Young healthy mice could therefore be analysed for glucose tolerance. Moreover, macrophages
241 and adipocytes, the other targets of VAT Tregs, remain microRNA sufficient in these mice.
242 *Drosha*^{lox/lox} lacking the CD4-cre transgene were analysed as controls. We previously showed that
243 *Drosha*^{lox/lox} mice are indistinguishable from wildtype mice or mice only harbouring the CD4-cre
244 transgene²⁰.

245

246 *Drosha* CD4-cre and control mice were fed on a normal chow or HFD for eight weeks from
247 weaning then subjected to glucose tolerance testing. Somewhat unexpectedly, there was no

248 difference between the response of Drossha CD4-cre and control mice, both in males and females,
249 and whether fed on normal chow or a HFD, but high-fat feeding impaired glucose responses in all
250 mice (Figure 6).

251

252 **T cell specific DROSHA deficiency results in a loss of both VAT Treg and conventional T cells**

253 We next analysed the Treg and conventional T cell compartments in the VAT of Drossha CD4-cre
254 mice. We previously showed that there is a 50% reduction in both Treg and conventional T cell
255 populations in the lymphoid organs of these mice ²⁰. Consistent with this, total VAT Tregs were
256 reduced by approximately half in Drossha CD4-cre mice, in both males and females, and whether
257 fed on normal chow or a HFD (FIG 7A). Both thymic-derived and peripherally induced VAT Tregs
258 were equally affected by DROSHA deficiency (Supplementary figure 3). However, while naïve
259 Tregs were lost, the frequency of terminally differentiated Tregs appeared largely unaffected
260 (Supplementary figure 3).

261

262 Compared to lymphoid organs ²⁰, the loss of conventional T cell populations was even more severe
263 in the VAT of Drossha CD4-cre mice (Figure 7b, c), with an almost total absence of CD8⁺ T cells, in
264 both male and female mice, and whether fed on normal chow or HFD. Thus, DROSHA deficiency
265 from the CD4⁺CD8⁺ stage in T cell development dramatically affects both Treg and conventional T
266 cell populations in the VAT but this does not alter responses to high-fat feeding. This suggests that
267 any impacts of microRNA deficiency on the metabolic function of VAT Tregs must be via the
268 interaction with conventional T cells rather than via direct interactions with macrophages or
269 adipocytes.

270 **DISCUSSION**

271 We have shown that expression of the miR-17~92a cluster of miRNAs by Tregs has a critical role
272 in metabolic control, with Treg-specific miR-17~92a deficiency rendering male mice resistant to
273 impaired blood glucose homeostasis caused by high-fat feeding. The metabolic functions of
274 adipose-resident Tregs is thought to involve complex interactions with other immune cells as well as
275 directly with adipocytes. In Treg-specific miR-17~92a deficient male mice, protection from high
276 feeding is likely to involve increased IL-10 and decreased IFN γ expression by conventional CD4⁺ T
277 cells.

278
279 IFN γ has pleiotropic impacts on adipose tissue function. It can directly act on adipocytes to inhibit
280 insulin signalling and to reduced lipid storage^{33,34}. Moreover, it inhibits the differentiation of pre-
281 adipocytes³³. IFN γ also promotes the polarization of macrophages towards a proinflammatory M1
282 phenotype that secrete other proinflammatory cytokines like TNF α to further inhibit insulin
283 signalling³⁵. Furthermore, the IFN γ in adipose tissues has been shown to inhibit Treg
284 differentiation and function³¹, which ultimately contributes to a feedback loop between
285 conventional T cell and Tregs that promotes adipose inflammation. Thus, the reduced IFN γ
286 expression in the VAT of miR-17~92a deficient male mice is likely to contribute to the protection
287 from a high-fat diet.

288
289 IL-10 is anti-inflammatory cytokine that is thought to suppresses adipose tissue inflammation and
290 insulin resistance³⁶. This may be occurring via its action on various immune cell types, such as by
291 suppressing conventional CD4⁺ and CD8⁺ T cell function³⁷. IL-10 has also been shown to inhibit
292 the expression of TNF α -induced pro-inflammatory genes in adipocytes, including chemokines like
293 CCL5 that would otherwise recruit other pro-inflammatory cells to the tissue⁶. Furthermore, IL-10
294 prevents TNF α from inhibiting insulin signalling in adipocytes⁶. Paradoxically, however, IL-10
295 also has been shown to repress the expression of thermogenic genes in adipocytes to promote lipid
296 storage³⁸. Tregs, M2 macrophages and conventional T cells have all been shown to be sources of
297 IL-10 in adipose tissue³⁵. The IL-10 produced by Tregs appears to contribute to insulin resistance
298 by directly acting on adipocytes to suppress thermogenesis³⁹. Thus, it could be that the
299 consequences of IL-10 in adipose tissue depends on both source and target. Clearly, the roles that
300 IL-10 plays in metabolic homeostasis are complex and remain to be clarified.

301
302 Regardless of these complex cytokine-cell interactions, high levels of IL-10 do appear to have a
303 therapeutic benefit. Administration of IL-10 improves insulin sensitivity and glucose tolerance
304 following high-fat feeding^{6,7}. Thus, the elevated IL-10 expression by conventional CD4⁺ T cells in

305 the VAT of miR-17~92a deficient male mice is also likely to contribute to the protection of these
306 mice from a high-fat diet.

307

308 The increased IL-10 and decreased IFN γ expression by VAT CD4⁺ T cells resulting from Treg-
309 specific miR-17~92a deficiency occurred in male but not female mice. Sexual dimorphism in VAT
310 Tregs has been reported previously¹⁰. The greater numbers of Tregs found in the VAT of male
311 mice than in that of female mice appears to be dependent on the androgen-regulated differentiation
312 of adipose stromal cells that produce IL-33¹⁰. The impact of miR-17~92a deficiency in the Tregs of
313 male mice could simply be due to males having a larger number of these cells. However, it may
314 also be related to the direct actions of the sex hormones on the Tregs themselves. Both androgen
315 and estrogen can directly signal Tregs^{40, 41}. The interaction of sex hormones with adipose tissue
316 cells is almost certainly involved in the male-specific impact miR-17~92a deficiency on glucose
317 responses because there was no difference in the impact of miR-17~92a deficiency on lymphoid
318 Tregs between male and female mice²⁶. Thus, miR-17~92a deficiency may be interacting with one
319 or both hormones, which then manifests as a differential resistance to a high-fat diet.

320

321 EOS is a zinc finger transcription factor that is an essential coregulator of FOXP3-mediated gene
322 transcription and the mRNA encoding this factor has been shown to be a target of miR-17²⁷. This
323 could potentially be a contributing mechanism in VAT Tregs but miR-17 along with the other
324 miRNAs in this cluster regulates numerous targets. In conventional CD4⁺ T cells, miR-17 has been
325 shown to regulate the *Tgfb2* and *Creb1* mRNAs, while miR-19b regulates *Pten*⁴². Whether these
326 are also targets in Tregs remains to be determined. Together, these suggest it is quite possible that
327 the miR-17~92a cluster operates as an inhibitor of the suppressor functions of VAT-resident Tregs.

328

329 Deletion of the *Mir17hg* gene in Tregs has also been shown to impair their function, that is, miR-
330 17~92a is required for the suppressor function of Tregs. We showed that the fitness of lymphoid
331 Tregs is impaired by miR-17~92a deficiency²⁶. Another study showed that mice with Treg-specific
332 miR-17~92a deficiency develop more severe disease in the experimental autoimmune
333 encephalomyelitis model of multiple sclerosis²⁵. This was associated with impaired differentiation
334 of naïve Tregs into IL-10-expressing effector Tregs. Thus, the role of miR-17~92a in Tregs appears
335 to be dependent on physiologic context. To understand the molecular mechanism underlying the
336 protection of Treg-specific miR-17~92a deficient male mice from high-fat feeding, it will be
337 important in future studies to determine the targets of miR-17~92a miRNAs in specifically within
338 VAT Tregs.

339 **METHODS**

340 **Mice**

341 Treg specific miR-17~92a deficient mice have been described previously ²⁶, which harbour a
342 conditional *Mir17hg^{lox}* allele and *Foxp3^{IRE5-Cre}* knockin. Control animals were generated by crossing
343 Treg specific miR-17~92a male mice with wildtype female mice to produce offspring with the
344 genotype *Mir17hg^{lox/+} Foxp3^{IRE5-Cre/+}* or *Mir17hg^{lox/+} Foxp3^{Y/+}*. *Drosha^{lox/lox} CD4-cre* mice have
345 been previously described ²⁰. They were crossed to *Foxp3^{IRE5-GFP}* knockin mice ³², which allowed
346 for identification of Tregs by expression of GFP.

347
348 Mice were fed with standard chow pellets or modified high fat pellets (diet SF01-025, Specialty
349 Feeds, Glen Forrest) *ad libitum* from weaning for eight weeks before analysis. The total fat content
350 of the high-fat diet was 22.3%, compared to 4.8% of the normal chow diet. The calculated energy of
351 the high-fat diet was 14.3 MJ Kg⁻¹ compared to 18.3 MJ Kg⁻¹ of the normal chow diet.

352
353 The mice were housed at St Vincent's Hospital Melbourne's BioResources Centre. Experiments
354 were approved by the Animal Ethics Committee of St Vincent's Hospital Melbourne and performed
355 under the Australian code for the care and use of animals for scientific purposes.

356

357 **Glucose tolerance testing**

358 A 30% w/v glucose (Sigma-Aldrich, St Louis) solution in sterile water was prepared fresh for each
359 experiment. The mice were fasted for 6 h, then a blood glucose reading was taken by nicking the
360 end of the tail with a scalpel blade to obtain a drop of blood. Mice were subsequently weighed and
361 injected intraperitoneally with a 2g kg⁻¹ bolus of glucose. Blood glucose readings were then taken at
362 15, 30, 45, 60, 75, 90 and 120 min after the glucose injection by warming the tail nick under a heat
363 lamp.

364

365 **VAT preparations**

366 To obtain leukocytes from visceral adipose tissue, the tissue was cut into small pieces with scissors
367 and digested with collagenase B (Sigma-Aldrich, St Louis) in RPMI (Sigma-Aldrich, St Louis) at
368 37°C for 20 min in a shaking incubator (at 200rpm). The digest was then filtered through a 70µm
369 strainer and washed twice with cold PBS (Sigma-Aldrich, St Louis). If required, red blood cells
370 were removed by treating the pellet with RBC lysis buffer (Thermo Fisher Scientific, Waltham)
371 between the two washes. The cells were then resuspended in RPMI + 10% FCS (GE Healthcare
372 Life Sciences, Chicago), filtered again through a 70µm strainer and allowed to recover at 37°C for
373 1h before antibody staining. For intracellular cytokine analyses, the cells were allowed to recover in

374 RPMI + 10% FCS supplemented with 50ng mL⁻¹ phorbol 12-myristate 13-acetate (Thermo Fisher
375 Scientific, Waltham), 1µg mL⁻¹ ionomycin (Thermo Fisher Scientific, Waltham) and Protein
376 Transport Inhibitor Cocktail (Thermo Fisher Scientific, Waltham) for 4h prior to antibody staining.

377

378 **Flow cytometry**

379 For the analysis of leukocytes from Mir17hg Foxp3-cre mice, the cells were first stained with
380 antibodies against cell surface antigens, before fixing and staining with an anti-FOXP3 antibody
381 using the FOXP3 / Transcription Factor Staining Buffer Set (Thermo Fisher Scientific, Waltham).

382 For the analysis of intracellular cytokine expression, the cells were first stained antibodies against
383 cell surface antigens, before fixing and staining with antibodies against cytokines using the
384 Intracellular Fixation and Permeabilization Buffer Set (Thermo Fisher Scientific, Waltham). The
385 cells were then resuspended in PBS 0.5% BSA 2mM EDTA for analysis. For the analysis of
386 leukocytes from Drosha CD4-Cre mice, the cells were simply stained with antibodies against cell
387 surface antigens in PBS 0.5% BSA 2mM EDTA (Sigma-Aldrich, St Louis). All antibodies used
388 were purchased from (Thermo Fisher Scientific, Waltham) and are listed in Supplementary table 1.
389 Data acquisition was performed on an LSRFortessa (BD Biosciences, Franklin Lakes) then
390 analysed on FlowJo ver10.7 (Ashland).

391

392 **Statistical analyses**

393 All statistical analyses were performed on Prism ver9 (GraphPad, San Diego). Comparisons
394 between multiple groups (male versus female and genotype) were assessed by ANOVA with
395 Tukey's *post hoc* test. Two-way comparisons were analysed by a *t*-test.

396 **ACKNOWLEDGMENTS**

397 The authors thank St Vincent's Hospital Melbourne's BioResources Centre's Vicki Moshovakis
398 and Rhiannon Walder for assistance with the glucose tolerance tests and Lucy Kloboucnik and
399 Vincent Madafferi for expert animal husbandry.

400

401 This work was funded by grants from the National Health and Medical Research Council
402 (GNT1122384 and GNT1122395), Diabetes Australia (Y20G-CHOM) and the U.S. Department of
403 Defense (W81XWH-19-1-0728). MMWC is a Senior Research Fellow of the National Health and
404 Medical Research Council. This work was made possible through Victorian State Government
405 Operational Infrastructure Support and Australian National Health and Medical Research Council
406 Research Institute Infrastructure Support Schemes.

407 **REFERENCES**

- 408 1. Tsiloulis T, Watt MJ. Exercise and the Regulation of Adipose Tissue Metabolism. *Prog Mol*
409 *Biol Transl Sci* 2015; **135**: 175-201.
- 410 2. Schipper HS, Prakken B, Kalkhoven E, Boes M. Adipose tissue-resident immune cells: key
411 players in immunometabolism. *Trends Endocrinol Metab* 2012; **23**: 407-415.
- 412 3. Munoz-Rojas AR, Mathis D. Tissue regulatory T cells: regulatory chameleons. *Nat Rev*
413 *Immunol* 2021; **21**: 597-611.
- 414 4. Bacchetta R, Passerini L, Gambineri E, *et al.* Defective regulatory and effector T cell
415 functions in patients with FOXP3 mutations. *J Clin Invest* 2006; **116**: 1713-1722.
- 416 5. Povoleri GA, Scotta C, Nova-Lamperti EA, John S, Lombardi G, Afzali B. Thymic versus
417 induced regulatory T cells - who regulates the regulators? *Front Immunol* 2013; **4**: 169.
- 418 6. Feuerer M, Herrero L, Cipolletta D, *et al.* Lean, but not obese, fat is enriched for a unique
419 population of regulatory T cells that affect metabolic parameters. *Nat Med* 2009; **15**: 930-
420 939.
- 421 7. Winer S, Chan Y, Paltser G, *et al.* Normalization of obesity-associated insulin resistance
422 through immunotherapy. *Nat Med* 2009; **15**: 921-929.
- 423 8. Cipolletta D, Cohen P, Spiegelman BM, Benoist C, Mathis D. Appearance and
424 disappearance of the mRNA signature characteristic of Treg cells in visceral adipose tissue:
425 age, diet, and PPAR γ effects. *Proc Natl Acad Sci U S A* 2015; **112**: 482-487.
- 426 9. Pettersson US, Walden TB, Carlsson PO, Jansson L, Phillipson M. Female mice are
427 protected against high-fat diet induced metabolic syndrome and increase the regulatory T
428 cell population in adipose tissue. *PLoS One* 2012; **7**: e46057.
- 429 10. Vasanthakumar A, Chisanga D, Blume J, *et al.* Sex-specific adipose tissue imprinting of
430 regulatory T cells. *Nature* 2020; **579**: 581-585.
- 431 11. Bapat SP, Myoung Suh J, Fang S, *et al.* Depletion of fat-resident Treg cells prevents age-
432 associated insulin resistance. *Nature* 2015; **528**: 137-141.
- 433 12. DiSpirito JR, Zemmour D, Ramanan D, *et al.* Molecular diversification of regulatory T cells
434 in nonlymphoid tissues. *Sci Immunol* 2018; **3**.
- 435 13. Cipolletta D, Feuerer M, Li A, *et al.* PPAR- γ is a major driver of the accumulation and
436 phenotype of adipose tissue Treg cells. *Nature* 2012; **486**: 549-553.
- 437 14. Siersbaek R, Nielsen R, Mandrup S. PPAR γ in adipocyte differentiation and metabolism--
438 novel insights from genome-wide studies. *FEBS Lett* 2010; **584**: 3242-3249.
- 439 15. Onodera T, Fukuhara A, Jang MH, *et al.* Adipose tissue macrophages induce PPAR γ -high
440 FOXP3⁺ regulatory T cells. *Sci Rep* 2015; **5**: 16801.

- 441 16. Frias AB, Jr., Hyzny EJ, Buechel HM, *et al.* The Transcriptional Regulator Id2 Is Critical
442 for Adipose-Resident Regulatory T Cell Differentiation, Survival, and Function. *J Immunol*
443 2019; **203**: 658-664.
- 444 17. Sullivan JM, Hollbacher B, Campbell DJ. Cutting Edge: Dynamic Expression of Id3
445 Defines the Stepwise Differentiation of Tissue-Resident Regulatory T Cells. *J Immunol*
446 2019; **202**: 31-36.
- 447 18. Vasanthakumar A, Moro K, Xin A, *et al.* The transcriptional regulators IRF4, BATF and IL-
448 33 orchestrate development and maintenance of adipose tissue-resident regulatory T cells.
449 *Nat Immunol* 2015; **16**: 276-285.
- 450 19. Johanson TM, Skinner JP, Kumar A, Zhan Y, Lew AM, Chong MM. The role of
451 microRNAs in lymphopoiesis. *Int J Hematol* 2014; **100**: 246-253.
- 452 20. Chong MM, Rasmussen JP, Rudensky AY, Littman DR. The RNaseIII enzyme Drosha is
453 critical in T cells for preventing lethal inflammatory disease. *J Exp Med* 2008; **205**: 2005-
454 2017.
- 455 21. Liston A, Lu LF, O'Carroll D, Tarakhovsky A, Rudensky AY. Dicer-dependent microRNA
456 pathway safeguards regulatory T cell function. *J Exp Med* 2008; **205**: 1993-2004.
- 457 22. Zhou X, Jeker LT, Fife BT, *et al.* Selective miRNA disruption in T reg cells leads to
458 uncontrolled autoimmunity. *J Exp Med* 2008; **205**: 1983-1991.
- 459 23. Cobb BS, Hertweck A, Smith J, *et al.* A role for Dicer in immune regulation. *J Exp Med*
460 2006; **203**: 2519-2527.
- 461 24. Kirigin FF, Lindstedt K, Sellars M, *et al.* Dynamic microRNA gene transcription and
462 processing during T cell development. *J Immunol* 2012; **188**: 3257-3267.
- 463 25. de Kouchkovsky D, Esensten JH, Rosenthal WL, Morar MM, Bluestone JA, Jeker LT.
464 microRNA-17-92 regulates IL-10 production by regulatory T cells and control of
465 experimental autoimmune encephalomyelitis. *J Immunol* 2013; **191**: 1594-1605.
- 466 26. Skinner JP, Keown AA, Chong MM. The miR-17~92a cluster of microRNAs is required for
467 the fitness of Foxp3⁺ regulatory T cells. *PLoS One* 2014; **9**: e88997.
- 468 27. Yang HY, Barbi J, Wu CY, *et al.* MicroRNA-17 Modulates Regulatory T Cell Function by
469 Targeting Co-regulators of the Foxp3 Transcription Factor. *Immunity* 2016; **45**: 83-93.
- 470 28. Yadav M, Louvet C, Davini D, *et al.* Neuropilin-1 distinguishes natural and inducible
471 regulatory T cells among regulatory T cell subsets *in vivo*. *J Exp Med* 2012; **209**: 1713-
472 1722, S1711-1719.
- 473 29. Cheng G, Yuan X, Tsai MS, Podack ER, Yu A, Malek TR. IL-2 receptor signaling is
474 essential for the development of Klrp1⁺ terminally differentiated T regulatory cells. *J*
475 *Immunol* 2012; **189**: 1780-1791.

- 476 30. Han JM, Wu D, Denroche HC, Yao Y, Verchere CB, Levings MK. IL-33 Reverses an
477 Obesity-Induced Deficit in Visceral Adipose Tissue ST2⁺ T Regulatory Cells and
478 Ameliorates Adipose Tissue Inflammation and Insulin Resistance. *J Immunol* 2015; **194**:
479 4777-4783.
- 480 31. Deng T, Liu J, Deng Y, *et al.* Adipocyte adaptive immunity mediates diet-induced adipose
481 inflammation and insulin resistance by decreasing adipose Treg cells. *Nature*
482 *Communications* 2017; **8**: 15725.
- 483 32. Bettelli E, Carrier Y, Gao W, *et al.* Reciprocal developmental pathways for the generation
484 of pathogenic effector TH17 and regulatory T cells. *Nature* 2006; **441**: 235-238.
- 485 33. McGillicuddy FC, Chiquoine EH, Hinkle CC, *et al.* Interferon γ attenuates insulin signaling,
486 lipid storage, and differentiation in human adipocytes via activation of the JAK/STAT
487 pathway. *J Biol Chem* 2009; **284**: 31936-31944.
- 488 34. Wentworth JM, Zhang JG, Bandala-Sanchez E, *et al.* Interferon- γ released from omental
489 adipose tissue of insulin-resistant humans alters adipocyte phenotype and impairs response
490 to insulin and adiponectin release. *Int J Obes (Lond)* 2017; **41**: 1782-1789.
- 491 35. Appari M, Channon KM, McNeill E. Metabolic Regulation of Adipose Tissue Macrophage
492 Function in Obesity and Diabetes. *Antioxid Redox Signal* 2018; **29**: 297-312.
- 493 36. Clementi AH, Gaudy AM, van Rooijen N, Pierce RH, Mooney RA. Loss of Kupffer cells in
494 diet-induced obesity is associated with increased hepatic steatosis, STAT3 signaling, and
495 further decreases in insulin signaling. *Biochim Biophys Acta* 2009; **1792**: 1062-1072.
- 496 37. Smith LK, Boukhaled GM, Condotta SA, *et al.* Interleukin-10 Directly Inhibits CD8⁺ T Cell
497 Function by Enhancing N-Glycan Branching to Decrease Antigen Sensitivity. *Immunity*
498 2018; **48**: 299-312 e295.
- 499 38. Rajbhandari P, Thomas BJ, Feng AC, *et al.* IL-10 Signaling Remodels Adipose Chromatin
500 Architecture to Limit Thermogenesis and Energy Expenditure. *Cell* 2018; **172**: 218-233
501 e217.
- 502 39. Beppu LY, Mooli RGR, Qu X, *et al.* Tregs facilitate obesity and insulin resistance via a
503 Blimp-1/IL-10 axis. *JCI Insight* 2021; **6**: e140644.
- 504 40. Goodman WA, Bedoyan SM, Havran HL, Richardson B, Cameron MJ, Pizarro TT.
505 Impaired estrogen signaling underlies regulatory T cell loss-of-function in the chronically
506 inflamed intestine. *Proc Natl Acad Sci U S A* 2020; **117**: 17166-17176.
- 507 41. Walecki M, Eisel F, Klug J, *et al.* Androgen receptor modulates Foxp3 expression in
508 CD4⁺CD25⁺Foxp3⁺ regulatory T-cells. *Mol Biol Cell* 2015; **26**: 2845-2857.

509 42. Jiang S, Li C, Olive V, *et al.* Molecular dissection of the miR-17-92 cluster's critical dual
510 roles in promoting Th1 responses and preventing inducible Treg differentiation. *Blood* 2011;
511 **118**: 5487-5497.

513 **FIGURE CAPTIONS**

514 **Figure 1: Treg-specific miR-17~92a deficiency protects male mice from high fat-impaired**
515 **glucose tolerance.** Mir17hg Foxp3-cre and control mice were fed on normal chow or HFD for 8
516 weeks from weaning, then subjected to glucose tolerance testing. **(a)** Blood glucose (B.G.)
517 measurements (mean \pm S.D. of $n = 5$ or 6 mice per group analysed over 3 experiments) were taken
518 at the indicated times following injection of glucose. Area under curve (AUC, mean \pm S.D. shown)
519 of blood glucose levels comparing chow versus HFD-fed **(b)** male and **(c)** female mice ($C =$
520 control, $KO =$ Mir17hg Foxp3-cre). Blood glucose curves were assessed by ANOVA and AUC
521 were assessed by a t -test (* $P < 0.05$, ** $P < 0.005$ compared to littermate controls).

522
523 **Figure 2: miR-17~92a deficiency perturbs Treg subpopulations in the VAT of male but not**
524 **female mice.** Mir17hg Foxp3-cre and control mice were fed on normal chow for 8 weeks from
525 weaning, then the VAT was analysed for Treg populations by flow cytometry. Tregs were identified
526 by intracellular staining for FOXP3 protein. Shown are the frequencies of **(a)** total FOXP3⁺ Tregs,
527 **(b)** thymic-derived CD304⁺ Tregs and **(c)** peripheral induced CD304⁻ Tregs as a percentage of total
528 CD45⁺ leukocytes and the frequency of KLRG1⁺ terminally differentiated cells within the **(d)**
529 CD304⁺ thymic-derived subset and **(e)** CD304⁻ peripheral-induced subset. Each dot is an individual
530 animal ($n = 5$ – 10 mice per group analysed over 5 experiments), with means indicated by the lines.
531 Comparisons were assessed by ANOVA (***) $P < 0.0005$, only control versus knockout
532 comparisons are indicated).

533
534 **Figure 3: High-fat feeding depletes VAT Tregs regardless of miR-17~92a expression, but the**
535 **perturbations in Treg subpopulations caused by miR-17~92a deficiency are maintained.**
536 Mir17hg Foxp3-cre and control mice were fed on a HFD for 8 weeks from weaning, then the VAT
537 was analysed for Treg populations flow cytometry. Tregs were identified by intracellular staining
538 for FOXP3 protein. **(a)** The frequency of total FOXP3⁺ Tregs as a percentage of total CD45⁺
539 leukocytes comparing male to female, knockout to control and chow-fed to HFD-fed mice. The data
540 for chow-fed mice is derived from Figure 2. Each dot is an individual animal ($n = 4$ – 10 mice per
541 group), with means indicated by the lines. Shown are the frequencies of **(b)** thymic-derived CD304⁺
542 Tregs and **(c)** peripheral induced CD304⁻ Tregs as a percentage of total CD45⁺ leukocytes and the
543 frequency of KLRG1⁺ terminally differentiated cells within the **(d)** CD304⁺ thymic-derived subset
544 and **(e)** CD304⁻ peripheral-induced subset in HFD-fed mice. Each dot is an individual animal ($n =$
545 4 – 6 mice per group, analysed over 4 experiments), with means indicated by the lines. Comparisons
546 were assessed by ANOVA (** $P < 0.005$, *** $P < 0.0005$, only control versus knockout
547 comparisons are indicated).

548

549 **Figure 4: Treg-specific miR-17~92a deficiency results in an increase of conventional CD8⁺ T**
550 **cells in VAT.** Mir17hg Foxp3-cre and control mice were fed on normal chow or HFD for 8 weeks
551 from weaning, then the VAT was analysed for conventional T cell (TCR β ⁺FOXP3⁻) populations.
552 By flow cytometry. Shown are the frequencies of **(a)** CD4⁺ and **(b)** CD8⁺ T cells as a percentage of
553 total CD45⁺ leukocytes comparing male to female, knockout to control and chow-fed to HFD-fed
554 mice. Each dot is an individual animal (n = 4–10 mice per group, analysed over 5 experiments),
555 with means indicated by the lines. Comparisons were assessed by ANOVA (* *P* < 0.05, ** *P*
556 <0.005, only control versus knockout comparisons are indicated).

557

558 **Figure 5: Increased IL-10 expression by conventional CD4⁺ T cells and other cytokine**
559 **perturbations in the VAT of Treg-specific miR-17~92a deficient male mice.** Mir17hg Foxp3-cre
560 and control mice were fed on a HFD for 8 weeks from weaning, then the conventional T cell
561 (TCR β ⁺ FOXP3⁻) populations in the VAT were analysed for cytokine expression by flow
562 cytometry. Shown is a representative set of flow cytometric plots (out of 3 sets of mice analysed
563 over 3 experiments) for IL-10 versus IFN γ or IL-2 versus IFN γ expression by CD4⁺ and CD8⁺ T
564 cells in **(a)** male and **(b)** female mice (KO = Mir17hg Foxp3-cre). **(c)** The pooled data from the 3
565 sets of mice analysed. Each dot is an individual animal, with means indicated by the lines.
566 Comparisons were assessed by ANOVA (**p* <0.05, ***p*<0.005, ****p*<0.0005, only control versus
567 knockout comparisons are indicated). **(d)** The frequency of KLRG1⁺ effector CD8⁺ T cells as a
568 percentage of total CD45⁺ leukocytes in the VAT of mice. Each dot is an individual animal (n = 5–
569 10 mice per group), with means indicated by the lines. Comparisons were assessed by a *t*-test (* *P*
570 <0.05, ** *P* <0.005 compared to littermate controls).

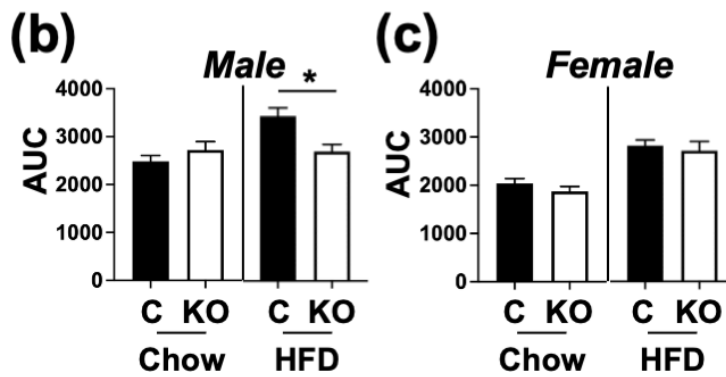
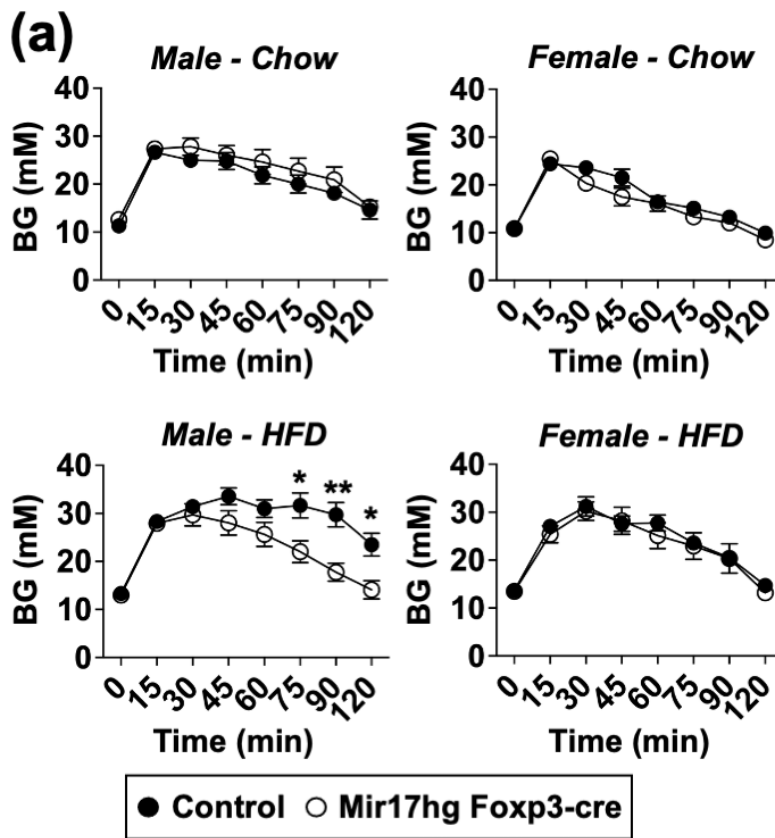
571

572 **Figure 6: Mice with DROSHA deficiency in all $\alpha\beta$ T cells exhibit normal responses to glucose**
573 **challenge.** Drosha CD4-cre and control mice were fed on normal chow or HFD for 8 weeks from
574 weaning, then subjected to glucose tolerance testing. **(a)** Blood glucose (B.G.) measurements (mean
575 \pm S.D. of n = 4–8 mice per group analysed over 4 experiments) were taken at the indicated times
576 following injection of glucose. Area under curve (AUC, mean \pm S.D. shown) of blood glucose
577 levels comparing chow versus HFD-fed **(b)** male and **(c)** female mice (C = control, KO = Drosha
578 CD4-cre). Blood glucose curves were assessed by ANOVA and AUC were assessed by a *t*-test (no
579 statistical difference found).

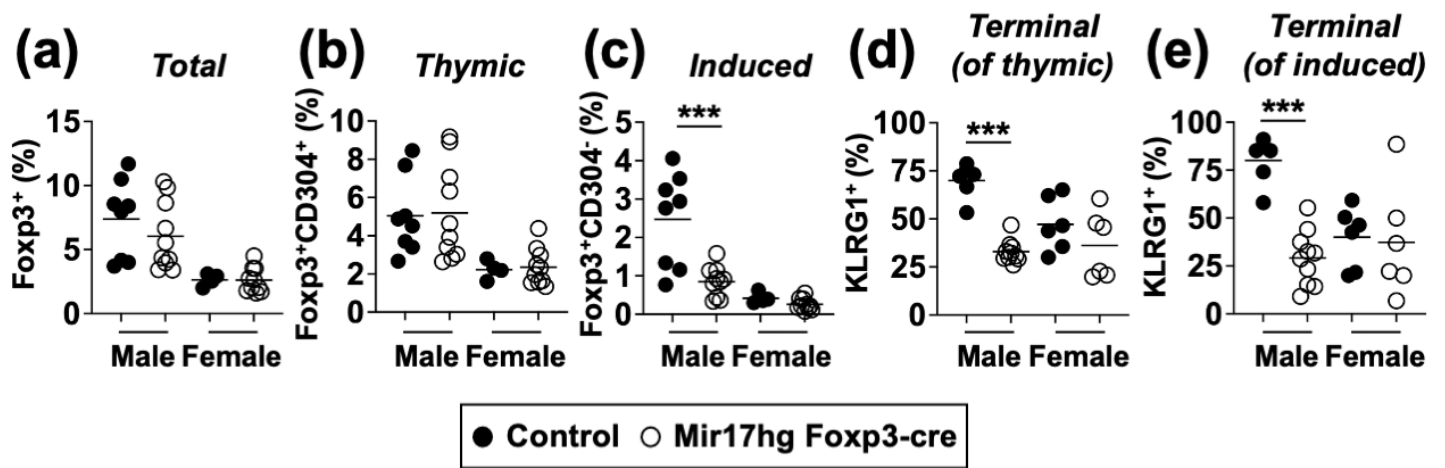
580

581 **Figure 7: Severe depletion of both Tregs and conventional T cells in the VAT of mice with**
582 **DROSHA deficiency in all $\alpha\beta$ T cells.** Drosha CD4-cre and control mice were fed on a normal

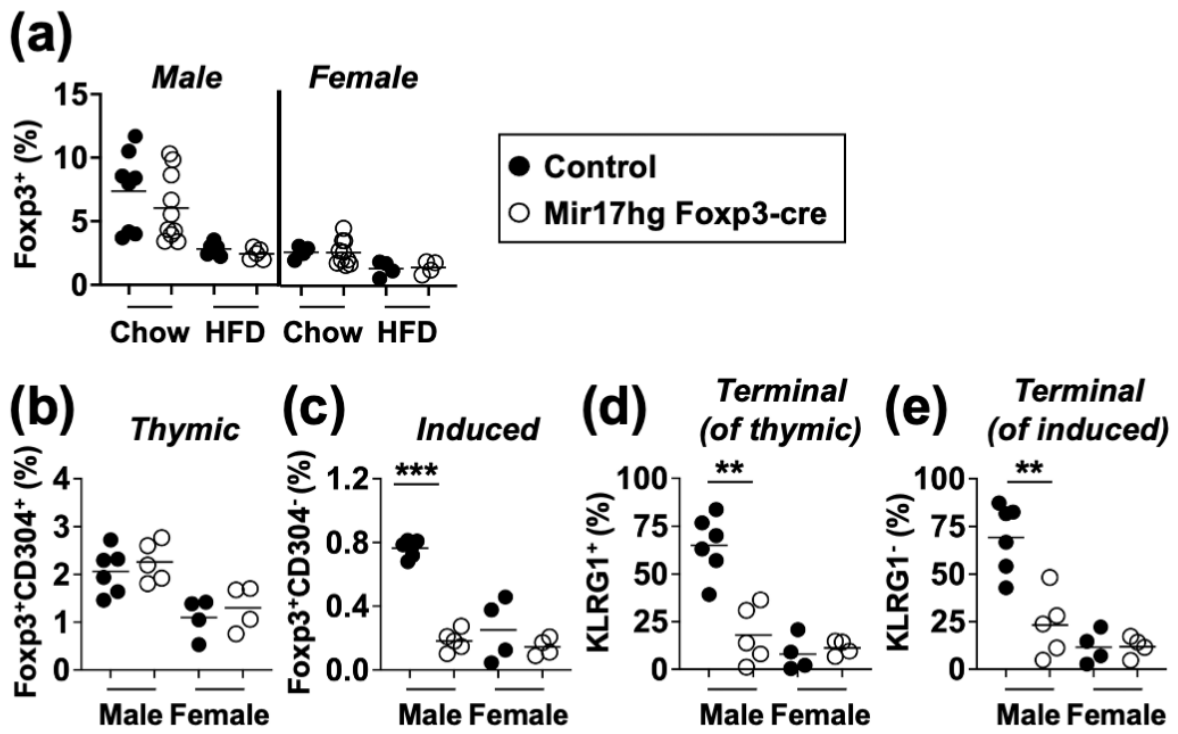
583 chow or HFD for 8 weeks from weaning, then the VAT was analysed for T cell populations by flow
584 cytometry. Tregs were identified by expression of a FOXP3-IRES-GFP reporter. Shown are the
585 frequencies of **(a)** total GFP(FOXP3)⁺ Tregs, **(b)** conventional CD4⁺(GFP⁻) and **(c)** CD8⁺(GFP⁻) T
586 cell populations as a percentage of total CD45⁺ leukocytes comparing male to female, knockout to
587 control and chow-fed to HFD-fed mice. Each dot is an individual animal (n = 4–7 mice per group
588 analysed over 4 experiments), with means indicated by the lines. Comparisons were assessed by
589 ANOVA (* $P < 0.05$, ** $P < 0.005$, *** $P < 0.0005$, only control versus knockout comparisons are
590 indicated).



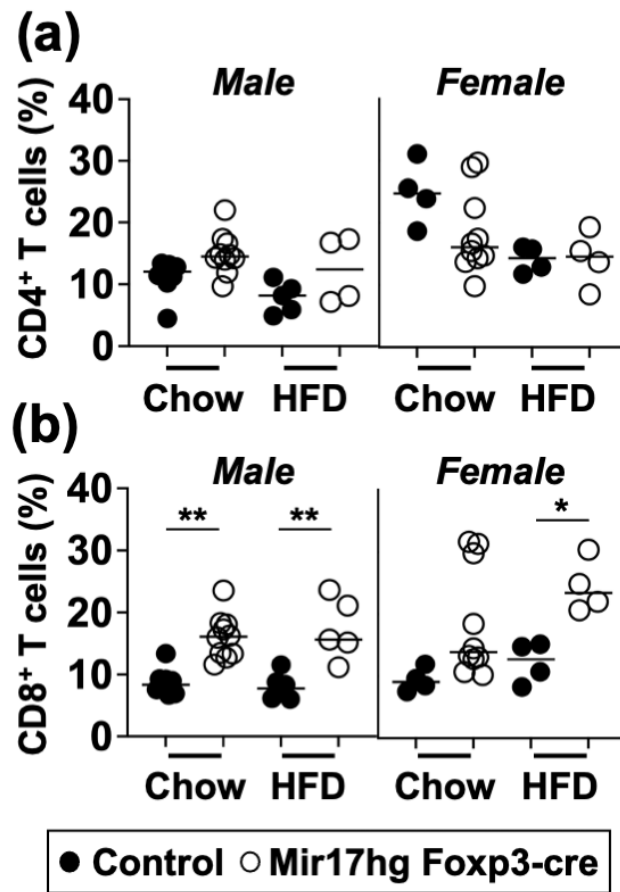
imcb_12513_f1.tiff



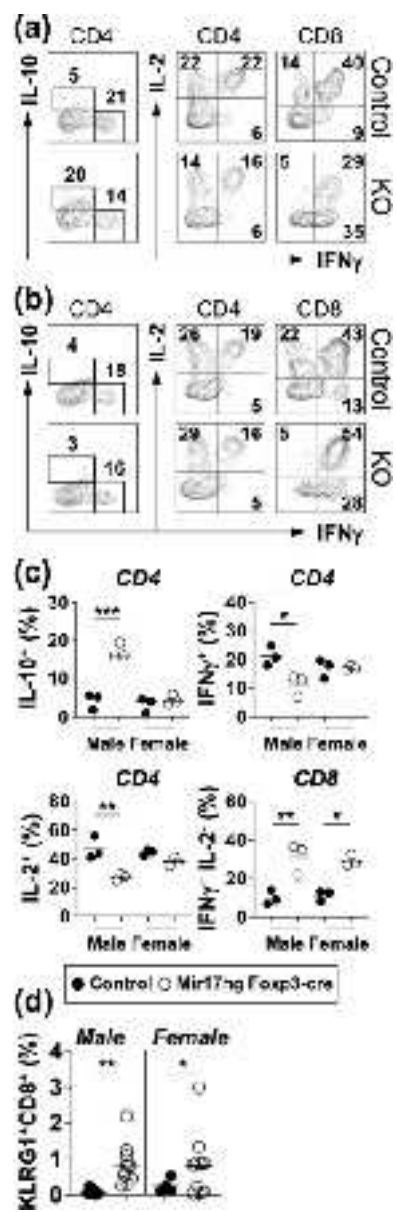
imcb_12513_f2.tiff



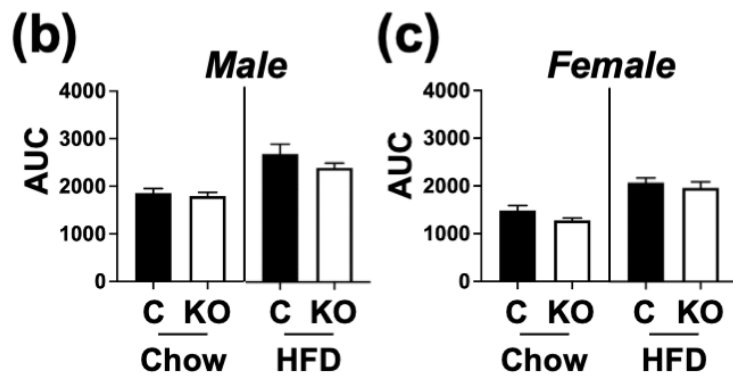
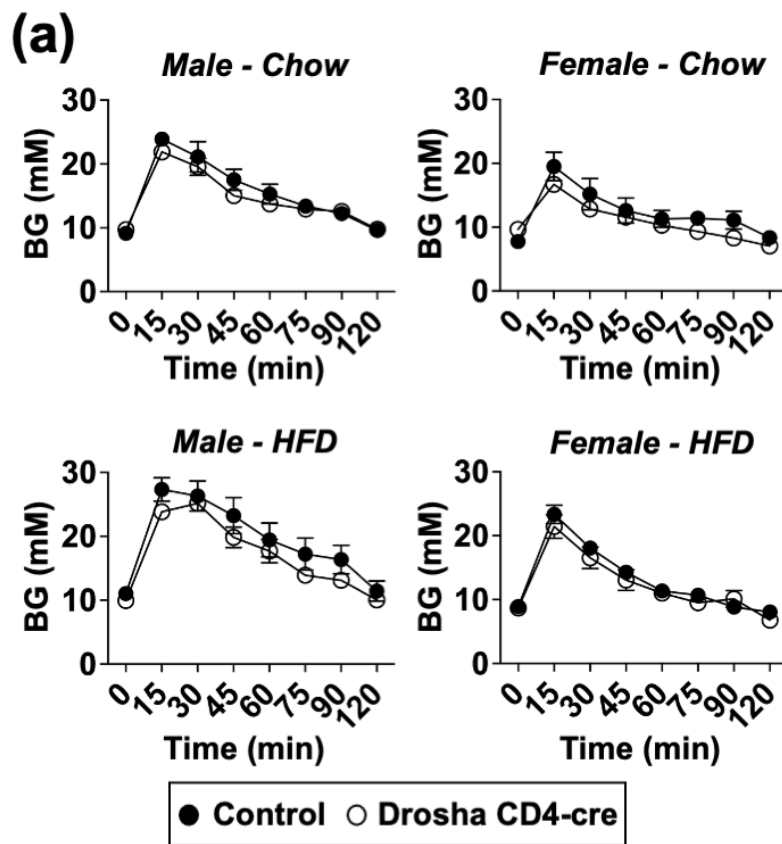
imcb_12513_f3.tiff



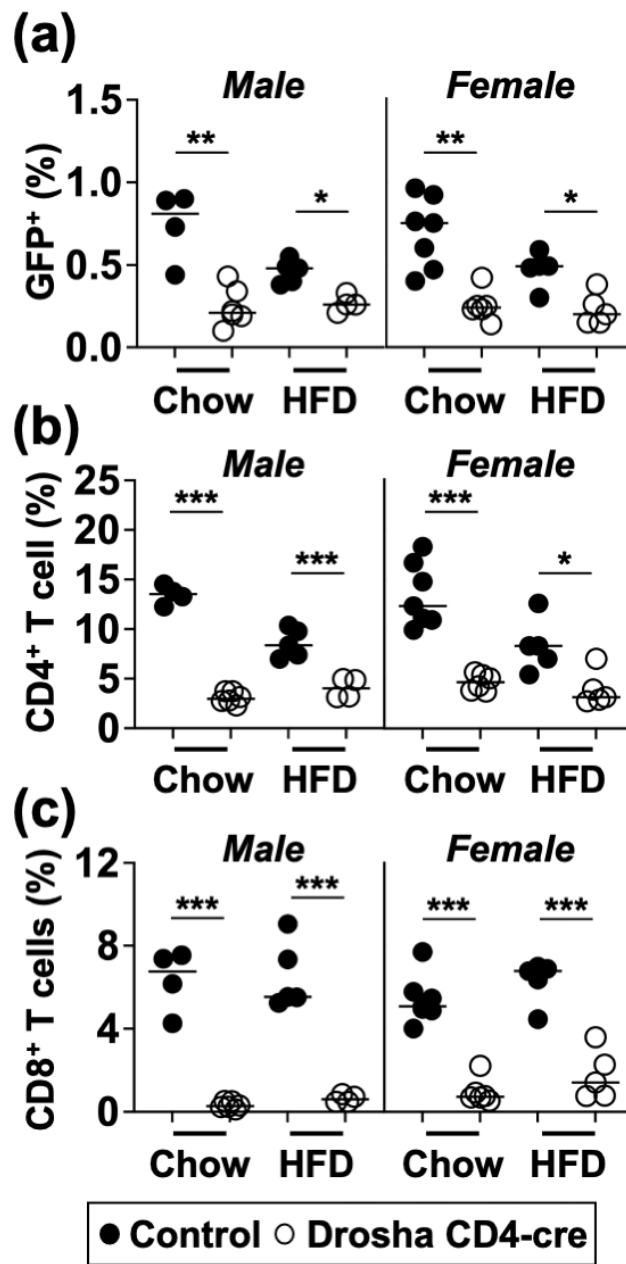
imcb_12513_f4.tiff



imcb_12513_f5.tiff



imcb_12513_f6.tiff



imcb_12513_f7.tiff